MaxEnt Machine Learning Technique based Assessment of Landslide Susceptibility of West Nayar Basin (Garhwal Himalaya), Uttarakhand, India

AJAY KUMAR

azai.geomatics99@hotmail.com

Soban Singh Jeena University https://orcid.org/0009-0006-5457-9515

Arvind Pandey

Soban Singh Jeena University

Atul Kumar

Chaudhary Charan Singh University

Research Article

Keywords: Landslide, Susceptibility, MaxEnt, West Nayar Basin (WNB), Uttarakhand, India

Posted Date: October 8th, 2024

DOI: https://doi.org/10.21203/rs.3.rs-4735597/v1

Abstract

Landslide susceptibility prediction mapping plays an imperative role in hazard mitigation by prioritizing areas for intervention and implementing effective risk reduction measures, thereby safeguarding communities and infrastructure. In this current assessment, 121 landslide occurrences and eight landslide-conditioning parameters were considered to develop a landslide susceptibility model for the West Nayar Basin (WNB), Uttarakhand, India. The Maximum Entropy multivariate statistical model (MaxEnt) was applied to calibrate and assess landslide susceptibility. The ensemble model data reveal that 2.69% and 7.31% of the WNB area are classified as very highly and highly susceptible to landslides, respectively. Meanwhile, around 65% of the basin is designated as a safe zone with a lower risk of landslides, and 25% of the area is identified as having a moderate probability of landslide risk. The major and frequent occurrence of landslides in the WNB is linked to low to middle elevations, proximity to rivers, and motorable roads. Consequently, the resulting model and observed patterns highlight the major variables that cause landslides and their corresponding significance. This modeling approach provides baseline data at a regional scale, which can enhance economic development planning in the WNB by informing better land use and watershed management practices. Integrating such models into planning processes ensures more resilient infrastructure and communities, promoting sustainable development in landslide-prone areas.

1. Introduction

Himalaya is a testament to the ongoing collision between the Indian and Eurasian plates, where tectonic upheavals have sculpted breathtaking landscapes and fostered unparalleled biodiversity. The Himalayas stand as one of the most precarious and delicate mountain regions on the globe, as noted in reference (Ives & Messerli, 2003). India's hilly landscapes stand as veritable hotbeds for landslides, with more than 12% of the nation's landmass perched precariously on the brink of this natural hazard. From the towering peaks of the northeast and northwest Himalayas to the rugged contours of the Western Ghats and the Eastern Ghats, these regions are particularly vulnerable to the ravages of landslides (Sarkar et al., 2006). The intricate interplay of myriad natural and human-induced activities, from the rugged contours of its slopes to the inconsistent rainfall patterns, the diverse lithology and geology, and the restless seismic activity, renders the Himalayan Mountains vulnerable to a myriad of natural hazards. Among these perils lie the specters of landslides, glacial lake outburst floods (GLOFs), the relentless creep of debris flows, and the ominous descent of ice and rock avalanches (Kaushik et al. 2020; Abdo 2022, Pandey et al. 2023). In the midst of climatic irregularities, landslides in the Himalayas have emerged as focal points of scientific inquiry, commanding attention for their capacity to unleash widespread devastation unlike any other natural hazard in the region (Das et al. 2023). However, the present conundrum lies in the fact that these landslides are exacerbated by the relentless growth of infrastructure, road construction, and hydropower projects in the mountainous expanse of the Himalayas (Sarkar et al. 2011; Kundu and Patel 2019; Sangeeta and Singh 2023).

Recent occurrences of landslides have exacted a heavy toll, inflicting widespread devastation and tragic loss of life and property in the region (Das et al. 2023). In light of these calamitous events, implementing robust measures for landslide mitigation has become an urgent necessity to ensure the sustainability and resilience of the Himalayan ecosystem.

Landslide susceptibility mapping has evolved into a reliable tool, greatly enhanced by the latest advancements in remote sensing and GIS technology (Hearn and Hart 2019; Lee 2019; Rahman et al. 2022; Basharat et al. 2023). Indeed, this tool plays a crucial role in decision-making for mitigating risks associated with landslides. Consequently, the production of accurate landslide susceptibility maps has become indispensable for disaster risk reduction and early warning systems. Over the past decades, numerous successful attempts have been made to map landslides using various mathematical modeling algorithms. Methods employed in landslide susceptibility and environmental modeling assessment encompass a range of approaches, including Frequency Ratio (Wang et al. 2020; Shu et al. 2021), Evidential Belief Function (Zhao et al. 2022), Functional Tree and Naïve Bayes (Pham et al. 2017), Generalized Additive Modelling (Bordoni et al. 2020), Neuro-Fuzzy (Ghorbanzadeh et al. 2020), Fuzzy Logic (Hejazi et al. 2022), Multilayer Perception Neural Network and Weighted Overlay (Singh et al. 2019; Abdo et al. 2022; Naceur et al. 2022) etc. Although, the effectiveness of various landslide mapping approaches on susceptibility models hasn't been extensively investigated, it's evident that the reliability and practicality of output results are heavily influenced by the suitability of the chosen models and the availability and quality of data.

A number of statistical and mathematical models have been developed and employed in the forecasting the distribution of plant and animal species, aiding research in conservation biology, ecology and evolution (Zimmermann et al. 2010, Pandey et al 2023). Certainly, among the array of predictive models, the Maximum Entropy Algorithm (MaxEnt) stands out as one of the most popular and widely utilized tools across various disciplines, including ecology, biology, climatology, and hydrology. Its effectiveness in forecasting distribution patterns in geographic space has made it a cornerstone in research and decision-making processes (Phillips & Dudık 2008, Pandey et al 2023, Pramanik et al., 2021). Indeed, the MaxEnt method has found extensive application in the prediction of landslide susceptibility assessment. Its robustness and versatility make it well-suited for analyzing the complex interplay of various factors contributing to landslide occurrence, ultimately aiding in the identification of high-risk areas and informing effective mitigation strategies. (Sharma et al. 2020; Pandey et al. 2021; Rahman et al. 2021; Boussouf et al. 2023).

The focal point of this study was to evaluate the viability of predicting landslide-susceptible zones within the West Nayar Basin (WNB) through the utilization of the Maximum Entropy Algorithm to ensemble data. The objective is to predict areas devoid of current landslide evidence but potentially susceptible to future occurrences. In this modeling endeavor, the assumption was made that areas sharing uniform conditioning factors (such as lithology, topography, vegetation, etc.) with existing landslide sites are more likely to become potential landslide locations in the future. Employing an ensemble model can effectively reduce the variability and dispersion of predictions, leading to improved model performance.

Determining optimal thresholds is indeed crucial for identifying landslide-prone areas and composing effective landslide susceptibility maps. These thresholds help delineate areas with varying degrees of susceptibility, enabling better risk assessment and mitigation strategies. MaxEnt methods are applied to optimize thresholds of statistical models in animal and plant ecological studies, including maximizes (sensitivity + specificity)/2, maximizes Kappa, mean predicted probability, and minimizes the distances between ROC plots etc. (Weigel et al. 2008; Cantor et al. 1999; Pramanik et al, 2021). The outcomes of this study facilitate valuable insights into generating more impactful and precise landslide-prone areas, which decision-makers and land-use managers can easily utilize to mitigate the risks posed by landslides within the WNB.

2. Methodology

2.1 Study area

Geographically, the West Nayar Basin (WNB) spans from 29º 54´ 42.351´´ N to 30º 13´ 14.243 N and 29º 56´ 6.259´´ E to 30º 9´ 18.617´´ E, encompassing a total area of approximately 746.83 km^2 and attitudinally, the catchment ranges from 558 m to 2972 m (see Fig. 1). The basin's rugged terrain, severe climatic conditions, geological instability, and the tumultuous flow of streams and tributaries render it highly susceptible to natural hazards such as landslides and flash floods. These hazards, triggered by cloud bursts and heavy rainfall, often lead to significant loss of human lives and infrastructure. Situated in the north and northeast part of the Pauri Garhwal District of Uttarakhand, India, the Himalayan landscape of the WNB is administratively divided into the blocks of Thalisain, Pabau, Ekeshwar, and Kaljikhal. The basin experiences rainfall from the tropical monsoon during summers and from western disturbances in the winter season.

2.2 Inventory of landslides and background points

In this study, we employed the widely renowned Maximum Entropy Algorithm to ensemble data for predicting landslide susceptibility in the WNB. The methodological flowchart of the step-wise modeling process is depicted in Figure-2. Landslide occurrences were spatially recorded as point data across the entire basin using a Garmin 650 Oregon GPS device. Leveraging the ease of identification provided by freely available software like Google Earth (Slingsby and Slingsby, 2019), we utilized a very high-resolution Google Earth Pro image from 2020 to pinpoint the spatial locations of previously observed landslides within the WNB. Following the identification of all landslides within the investigation area, a comprehensive sampling approach was employed. Each identified landslide was meticulously marked, culminating in the pinpointing of a total of 121 potential landslide sites during ground verification.

Among them, a subset comprising 30% of randomly selected landslide sites was verified through ground-truthing (see Fig. 3) from December 2018 to August 2022, resulting in a accuracy assessment. Following the removal of spatial autocorrelations with the SDM toolbox (Brown, 2014), a total of 121 locations remained. Of the identified locations, 70% were randomly assigned as training points for the

development of landslide susceptibility models, while the remaining 30% were earmarked as test datasets to assess the performance of each model. Comprehensive field surveys were conducted to collect ground data and conduct on-site verification, ensuring the accuracy and reliability of the models. All the processing and calibrations regarding this assessment were conducted using ArcGIS Pro 3.0.1 (ESRI 2022). Likewise, 121 presence records were utilized for training purposes across the entirety of the West Nayar Basin (WNB) for the subsequent modeling endeavors. Additionally, a total of 10,105 points, randomly permuted by the algorithm, were employed for MaxEnt distribution processing, encompassing both background points and presence points.

2.3 Landslide Predictor Variable

Eight landslide predictor variables for landslide susceptibility assessment, viz., lithology, geomorphology, elevation, precipitation, river, drainage density, angle of slope and aspect (figure-4) have taken into the account.

2.4 Statistical Analysis of Correlation

The Pearson Correlation Coefficient (PCC or r) method was utilized to assess multicollinearity or pairwise correlation among all predictor variables using ArcGIS Pro 3.0.1 (Benesty et al., 2009). PCC values range from − 1 to 1, where a positive value indicates a perfect positive relationship between the variables, a negative value depicts a perfect negative relationship, and a null value signifies relatively no relationship among the variables (Guo et al., 2014). The PCC can be calculated using Eq. 1.

$$r_{xy} = \frac{\sum_{i=1}^{n}\left(x_i-\bar{x}\right)*\left(y_i-\bar{y}\right)}{\sqrt{\sum_{i=1}^{n}\left(x_i-\bar{x}\right)^2 \Sigma_{i=1}^{n}\left(y_i-\bar{y}\right)^2}} \quad \text{..... Eq. 1}$$

where, r_{xy} = Pearson Coefficient Correlation (PCC) between the variables *X* and *Y*. The x_i is the values for *X* variables, y_i values for *Y* variables, *x* stands for the average of the *X* variable samples and *y* is for the average of the *Y* values dataset.

2.4 Model Building: Maximum Entropy Model (MaxEnt)

The Maximum Entropy (MaxEnt) model is rooted in the entropy maximization principle of statistical physics (Banavar et al., 2010), originating from an information-theoretic approach (Ruddell et al., 2013) that is applicable to predicting spatiotemporal patterns of landslide occurrence. Initially employed in ecosystem studies to forecast species distribution using species occurrence data (Grimm et al., 2005; Phillips and Dudík, 2008), MaxEnt has gained popularity in various fields (Elith et al., 2011). However, its application in landslide susceptibility modeling has not been thoroughly explored (Felicísimo et al., 2013).

MaxEnt identifies potential sets of predictors from which a pattern might emerge. Subsequently, it utilizes sets of predictor variables and landslide occurrence data to collectively identify the most

'susceptible' conditions. In this case, eight categorical variables were selected as the most favorable predictors for predicting landslide-susceptible conditions using MaxEnt. The MaxEnt model, based on information theory and statistics, employs default parameters to estimate landslide probability values ranging from 0 to 1. It assigns importance weights to the sample area's locations, thus carving out the landslide distribution as a probability distribution (Felicísimo et al., 2013). By considering both the existence or absence of landslide sites, MaxEnt evaluates landslide probability distributions. Subsequently, employing the maximum entropy rule, it extends the distribution function to the most likely sites (Felicísimo et al., 2013). The primary aim of MaxEnt modeling is to find the Gibbs distribution that maximizes the probability of a given log-likelihood, which can be calculated using Eq. 2 (Phillips and Dudík, 2008; Park, 2015).

$$\frac{1}{m}\sum_{i=1}^{m} ln\left[q\lambda\ (x_i)\right] - \sum_{j=1}^{n}\beta_j\left|\lambda_i\right| \quad \text{..... Eq. 2}$$

Here, the term βj represents the normalization constant for the variables included for the jth features. The first term of the equation corresponds to the log probability function, which enhances data accuracy and maximizes the model's value. The second part of the equation represents the normalization value. It becomes apparent that the Gibbs distribution function, derived through MaxEnt modeling, provides the best fit for the data.

2.5 Model performance

In this analysis, the Receiver Operating Characteristic (ROC) Curve is utilized to assess the accuracy of statistical models (Chen et al., 2017, Pandey et al., 2020). This approach enables a diagnostic evaluation to differentiate between two independent events and evaluate the performance of the classifier (Swets, 1988). The curve illustrates the trade-off between the true-positive rate, representing the probability of correctly predicting an expected event, and the false-negative or false-positive rate, representing the probability of incorrectly predicting an event. The ROC Curve aids in calculating the future probabilities of landslide occurrence, providing insights into the model's quality and predictive capabilities (Brenning, 2005). Model accuracy, determined by the area under ROC curve (AUC), is computed, with values ranging from 0 to 1. AUC values near 1 indicate excellent model performance, while values around 0.5 suggest poor model performance (Boussouf et al., 2023; Pramanik et al. 2021; Pradhan, 2013).

2.6 Ensemble Model

The MaxEnt model has achieved an AUC value of 0.928, indicating the high reliability of the susceptibility maps. However, while the sensitivity map provides valuable information with values ranging from 0 to 1, it is often more practical for decision-makers to visualize the landscape in distinct categories, such as low, moderate, high and very highly susceptible to landslides. This kind of output, which incorporates a continuous susceptibility index, obviously conveys more information than a simple presence/absence map. It is more convenient for landslide management support because it allows for more nuanced risk assessment and prioritization of mitigation efforts. This approach enables stakeholders to better understand varying levels of risk across different areas, facilitating more informed decision-making and

resource allocation for landslide prevention and response (Wang et al., 2024). Real curves often exhibit steps or exponential patterns, underscoring the need for a method that objectively determines thresholds to reclassify susceptibility intensity into different classes. This approach enhances the accuracy of the landslide susceptibility map by providing clear distinctions between different levels of risk.

In the current assessment, the spatial layer of model output indicating the varying intensity of landslide susceptibility was reclassified into four classes. Predicted-to-expected ratios (Fi) for each category were then determined using Eq. 3.

$$F_i = \frac{P_i}{E_i} \quad \text{..... Eq. 3}$$

Where, Pi represents the expected frequency of assessment points in class i, while E_i signifies the expected frequency relative to the area covered by each class. E_i values were plotted against class intervals.

The output susceptibility spatial layer was reclassified in to four zones indicting very high, high, moderate and low susceptibility to landslide occurrence. The output spatial prediction of susceptibility was validated using ground-truthing data, showing that out of 121 locations, 80 (96.8%) accurately fell within the risk zone. The ensemble-derived landslide susceptibility map revealed that the areas most prone to landslides were concentrated along the lower valley zone at low to middle elevations, extending towards the southwestern region and along riverbanks. Higher elevation areas showed minimal landslide occurrences.

3. Results

3.1 Observed pattern of landslide occurrence

Entire WNB consists about 746.83 km^2 area that is classified into four zones indicting very high, high, moderate and low susceptibility to landslide occurrence in the river basin. Approximately 2.69% and 7.31% of the area were classified as very highly and highly susceptible to landslides, respectively. Meanwhile, about 65% of the basin was designated as a safe zone with a lower risk of landslides, and 25% of the area was identified as having a moderate probability of landslide risk. Figure 6 depicts the landslide susceptibility map, highlighting four distinct zones ranging from low to very high intensity of landslide occurrence in the West Nayar Basin, Uttarakhand, India.

The landslides occurrences were much more frequent in areas having a slop range of > 25° to < 30° and > 30.1° to < 70.68° with South-East, North, and North-East aspects, of which Western slopes were affected the most. The observed landslides had manifested primarily in Jaunsar Geologic Group, 55.37% landslides occurred in Phyllite, Quartzite, Shale, Dolomite, Tuff with Dolerite Lithologic group followed by Shale, Quartzite, Limestone and Conglomerate Lithologic Group (18.18%). The very high and high

susceptible areas receive a moderate range of precipitation 954–1600 mm annually, indicates its modest contribution in Jackknife test. The high presence of drainage density ranging (Dd) 1.81–4.08 is recorded in the very high to highly susceptible areas, show a moderate permutation importance. The high elevation range 1500.1–2972 m encompassing low and moderate susceptible zones, whereas, very high and highly susceptible zones fall majorly under the elevation ranges between 558 to 1000 m and 1000.1 to 1500 m respectively.

High permutation importance of lithology (32.2) and geomorphology (26.1) have shown in the (Table 1), subsequently have a major importance in the landslide occurrence. Detailed relative contribution and preferences of landslides regarding eight independent predictor variables are available in the (Table-1)

3.2 Model Outcome

The predictive performance of the MaxEnt algorithm is shown in Fig. 6(a). Following this, the ROC curve, which plots sensitivity (1 – Omission Rate) against 1 – Specificity (Fractional Predicted Area) for landslides, is displayed in Fig. 6 (b). The training data achieves an AUC of 0.928, while a random prediction yields an AUC of 0.5. Figure 7 highlights the contribution and influence of each category of different predictors in the MaxEnt model, as illustrated by the Jackknife of regularized training gain. It is evident that lithology, elevation, and river streams are the most significant environmental predictors, whereas slope and aspect have the least influence on the landslide susceptibility model developed using the MaxEnt algorithm. Figures 8(a)-(h) depict the response patterns of landslides to all environmental predictor variables.Figure 6 (a) Predictive Performance of MaxEnt Model (b) Receiver Operating Characteristic (ROC) Curve

3.3 Sensitivity and Response Curve Analysis

The sensitivity analysis was conducted to examine the relative strengths of each of the eight predictor variables on the predicted maps' outcomes, utilizing the Jackknife test. Table 1 presents the results of the Kappa-based Jackknife test, employing AUC on test data for landslides (Javidan et al., 2021).

Table 1
Relative Contributions of the Environmental Variables to the MaxEnt Model

Variable	Percent contribution	Permutation importance
River streams	25.5	8.5
Elevation	23.8	14.8
Lithology	21.2	32.2
Geomorphology	11.8	26.1
Drainage Density	10.4	12.9
Precipitation	3.3	0.6
Aspect	1.9	4.9
Slope	1.9	0

3.4 Analysis of Variable Contribution

Table 1 provides estimates of the relative contributions of various environmental variables to the MaxEnt model. The first estimate is derived by summing the increase in regularized gain associated with each variable during each iteration of the training algorithm; this increase is added to the variable's contribution if the change is positive, or subtracted if the change is negative. For the second estimate, the values of each environmental variable in the training presence and background data are randomly permuted, and the model is then reevaluated on this permuted data. The resultant decrease in training AUC, normalized to percentages, is presented in Table 1. This approach helps in understanding the significance of each variable in predicting landslide susceptibility.

All the participating landslide conditioning parameters and their predicted probability of presence have shown in the (figure-8). In the Y-axis the predicted probability of presence has shown. This is the probability that a participating variable obtained in model and present in West Nayar Basin amid landslide based on the environmental conditions, whereas, the X-axis represents the conditioning parameter being varied.

4. Conclusion

Both continuous and categorical datasets were employed to generate a landslide susceptibility map of the study area using the MaxEnt machine learning technique. The results indicate that approximately 2.69% and 7.31% of the area are classified as very highly and highly susceptible to landslides, respectively. Meanwhile, around 65% of the basin is designated as a safe zone with a lower risk of landslides, and 25% of the area is identified as having a moderate probability of landslide risk. The highly susceptible areas are concentrated in the southern, southwestern, and western parts of the basin.

This research demonstrates the applicability of the MaxEnt machine learning technique in other study areas for hazard mitigation, providing advanced facilities for insurance purposes and land use planning. Effective hazard mitigation requires a coordinated approach to align individual efforts with existing policies. Risk and hazard management considerations are essential prerequisites for disaster management. Utilizing the landslide susceptibility map and hazard-based probability mapping can serve as valuable tools to initiate and plan further land use activities and schemes, ensuring a more informed and strategic approach to land management and disaster preparedness.

Landslide susceptibility assessment not only aids in mitigating hazard risks but also provides stakeholders with vital information and a comprehensive understanding of landscape changes. Consequently, integrating landslide susceptibility assessment into comprehensive watershed management and land use planning initiatives enhances the strategic allocation of resources, improves disaster preparedness, and supports sustainable development. By incorporating these assessments, planners can better anticipate potential landslide events, prioritize areas for intervention, and implement effective risk reduction measures, thereby safeguarding communities and infrastructure.

Declarations

Conflicts of Interest:

The authors declare no conflict of interest. 341

Funding:

No funding has received for conducting this research.

References

1. Abdo HG (2022) Assessment of landslide susceptibility zonation using frequency ratio and statistical index: a case study of Al-Fawar basin, Tartous, Syria. Int J Environ Sci Technol 19(4):2599–2618. 10.1007/s13762-021-03322-
2. Banavar JR, Maritan A, Volkov I (2010) Applications of the principle of maximum entropy: from physics to ecology. J Phys Condens Matter 22(6):063101. 10.1088/0953-8984/22/6/063101
3. Basharat M, Khan JA, Abdo HG, Almohamad H (2023) An integrated approach-based landslide susceptibility mapping: case of Muzaffarabad region, Pakistan. Geomatics Nat Hazards Risk 14(1):2210255. 10.1080/19475705.2023.2210255
4. Benesty J, Chen J, Huang Y, Cohen I (2009) Pearson correlation coefficient. Noise reduction in speech processing. Springer, Berlin, Heidelberg, pp 1–4
5. Bordoni M, Galanti Y, Bartelletti C, Persichillo MG, Barsanti M, Giannecchini R, Avanzi GD, Cevasco A, Brandolini P, Galve JP et al (2020) The influence of the inventory on the determination of the rainfall-

induced shallow landslides susceptibility using generalized additive models. CATENA 193:104630doi. 10.1016/j.catena.2020.104630

6. Boussouf S, Fernández T, Hart AB (2023) Landslide susceptibility mapping using maximum entropy (MaxEnt) and geographically weighted logistic regression (GWLR) models in the Río Aguas catchment (Almería, SE Spain). Nat Hazards 117(1):207–235
7. Boussouf S, Fernández T, Hart AB (2023) Landslide susceptibility mapping using maximum entropy (MaxEnt) and geographically weighted logistic regression (GWLR) models in the Río Aguas catchment (Almería, SE Spain). Nat Hazards 117(1):207–235
8. Brenning A (2005) Spatial prediction models for landslide hazards: review, comparison and evaluation. Nat Hazards Earth Syst Sci 5(6):853–862. 10.5194/nhess-5-853-2005
9. Cantor SB, Sun CC, Tortolero-Luna G, Richards-Kortum R, Follen M (1999) A comparison of C/B ratios from studies using receiver operating characteristic curve analysis. J Clin Epidemiol 52(9):885–892. 10.1016/s0895-4356(99)00075-x
10. Chen W, Pourghasemi HR, Kornejady A, Zhang N (2017) Landslide spatial modeling: Introducing new ensembles of ANN, MaxEnt, and SVM machine learning techniques. Geoderma 305:314–327
11. Das S, Sarkar S, Kanungo DP (2023) A critical review on landslide susceptibility zonation: recent trends, techniques, and practices in Indian Himalaya. Nat Hazards 115(1):23–72. 10.1007/s11069-022-05554-x
12. Elith J, Phillips SJ, Hastie T, Dudık M, Chee YE, Yates CJ (2011) A statistical explanation of MaxEnt for ecologists. Divers Distrib 17(1):43–57. 10.1111/j.1472-4642.2010.00725.x
13. ArcGIS Pro: Version 3.0.1. Environmental Systems Research Institute [Computer software]. ESRI, Redlands CA (2022) Retrieved from https://www.esri.com/enus/arcgis/products/arcgis-pro/overview
14. Felicısimo AM, Cuartero A, Remondo J, Quiros E (2013) Mapping landslide susceptibility with logistic regression, multiple adaptive regression splines, classification and regression trees, and maximum entropy methods: a comparative study. Landslides 10(2):175–189. 10.1007/s10346-012-0320-1
15. Ghorbanzadeh O, Blaschke T, Aryal J, Gholaminia K (2020) A new GIS-based technique using an adaptive neuro-fuzzy inference system for land subsidence susceptibility mapping. J Spat Sci 65(3):401–418. 10.1080/14498596.2018.1505564
16. Grimm V, Revilla E, Berger U, Jeltsch F, Mooij WM, Railsback SF, Thulke HH, Weiner J, Wiegand T, DeAngelis DL (2005) Pattern-oriented modeling of agent-based complex systems: lessons from ecology. Science 310(5750):987–991. 10.1126/science.1116681
17. Guo W, Ni X, Jing D, Li S (2014) Spatial-temporal patterns of vegetation dynamics and their relationships to climate variations in Qinghai Lake Basin using MODIS time-series data. J Geogr Sci 24(6):1009–1021. 10.1007/s11442-014-1134-y
18. Hearn GJ, Hart AB (2019) Landslide susceptibility mapping: a practitioner's view. Bull Eng Geol Environ 78:5811–5826

19. Hejazi A, Javadi M, Musavi Kojabad N (2022) Landslide Hazard Evaluation and Zoning with Fuzzy Logic (Case Study: Saraju River Basin). Geography (Regional Planning). (Hejazi, 2022)
20. Ives JD, Messerli B (2003) The Himalayan dilemma: reconciling development and conservation. Routledge
21. Javidan N et al (2021) Evaluation of Multi-Hazard Map Produced using MaxEnt Machine Learning Technique. Scientific Reports (2021) 11:6496 doi.org/10.1038/s41598-021-85862-7
22. Kaushik S, Rafiq M, Joshi PK, Singh T (2020) Examining the glacial lake dynamics in a warming climate and GLOF modelling in parts of Chandra basin, Himachal Pradesh, India. Sci Total Environ 714:136455. 10.1016/j.scitotenv.2019.136455
23. Kundu V, Patel RC (2019) Susceptibility status of landslides in Yamuna valley, Uttarakhand, NW-Himalaya, India. Him Geol 40(1):30–49
24. Lee S (2019) Current and future status of GIS-based landslide susceptibility mapping: a literature review. Korean J Remote Sens 35(1):179–193
25. Naceur HA, Abdo HG, Igmoullan B, Namous M, Almohamad H, Al Dughairi AA, Al-Mutiry M (2022) Performance assessment of the landslide susceptibility modelling using the support vector machine, radial basis function network, and weight of evidence models in the N'fis river basin, Morocco. Geosci Lett 9(1):39. 10.1186/s40562-022-00249-4
26. Naimi B, Araujo MB (2016) sdm: a reproducible and extensible R platform for species distribution modelling. Ecography 39(4):368–375. 10.1111/ecog.01881
27. Pandey A, Shekhar Sarkar M, Palni S, Parashar D, Singh G, Kaushik S, Chandra N, Costache R, Singh P, Pratap A, Mishra A, Almohamad H (2023) Multivariate statistical algorithms for landslide susceptibility assessment in Kailash Sacred landscape, Western Himalaya. Geomatics, Natural Hazards and Risk, 14(1), p.2227324
28. Pandey VK, Pourghasemi HR, Sharma MC (2020) Landslide susceptibility mapping using maximum entropy and support vector machine models along the Highway Corridor, Garhwal Himalaya. Geocarto Int 35(2):168–187
29. Pandey VK, Pourghasemi HR, Sharma MC (2020) Landslide susceptibility mapping using maximum entropy and support vector machine models along the Highway Corridor, Garhwal Himalaya. Geocarto Int 35(2):168–187
30. Park NW (2015) Using maximum entropy modeling for landslide susceptibility mapping with multiple geoenvironmental data sets. Environ Earth Sci 73(3):937–949. 10.1007/s12665-014-3442-z
31. Pham BT, Bui DT, Pourghasemi HR, Indra P, Dholakia MB (2017) Landslide susceptibility assessment in the Uttarakhand area (India) using GIS: a comparison study of prediction capability of naïve bayes, multilayer perceptron neural networks, and functional trees methods. Theor Appl Climatol 128(1–2):255–273. 10.1007/s00704-015-1702-9
32. Phillips SJ, Dudık M (2008) Modeling of species distributions with Maxent: new extensions and a comprehensive evaluation. Ecography 31(2):161–175. 10.1111/j.0906-7590.2008.5203.x

33. Pradhan B (2013) A comparative study on the predictive ability of the decision tree, support vector machine and neuro-fuzzy models in landslide susceptibility mapping using GIS. Comput Geosci 51:350–365. 10.1016/j.cageo.2012.08.023
34. Pramanik M, Diwakar AK, Dash P, Szabo S, Pal I (2021) Conservation planning of cash crops species (Garcinia gummi-gutta) under current and future climate in the Western Ghats, India. Environ Dev Sustain 23(4):5345–5370
35. Rahaman A, Venkatesan MS, Ayyamperumal R (2021) GIS-based landslide susceptibility mapping method and Shannon entropy model: a case study on Sakaleshapur Taluk, Western Ghats, Karnataka, India. Arab J Geosci 14:1–12
36. Rahman G, Bacha AS, Ul Moazzam MF, Rahman AU, Mahmood S, Almohamad H, Al Dughairi AA, Al-Mutiry M, Alrasheedi M, Abdo HG (2022) Assessment of landslide susceptibility, exposure, vulnerability, and risk in Shahpur Valley, eastern Hindu Kush. Front Earth Sci 10:1348. 10.3389/feart.2022.953627
37. Ruddell BL, Brunsell NA, Stoy P (2013) Applying information theory in the geosciences to quantify process uncertainty, feedback, scale. Eos Trans AGU 94(5):56–56. 10.1002/2013EO050007
38. Sangeeta SSK (2023) Influence of anthropogenic activities on landslide susceptibility: a case study in Solan district, Himachal Pradesh, India. J Mt Sci 20(2):429–447. 10.1007/s11629-022-7593-1
39. Sarkar S, Kanungo DP, Chauhan PKS (2011) Varunavat landslide disaster in Uttarkashi,Garhwal Himalaya, India. QJEGH 44(1):17–22. 10.1144/1470-9236/09-029
40. Sarkar S, Kanungo DP, Patra AK (2006) Landslides in the Alaknanda Valley of Garhwal Himalaya, India. Q J Eng GeolHydrogeol 39(1):79–82
41. Sharma A, Prakash C, Manivasagam VS (2021) Entropy-based hybrid integration of random forest and support vector machine for landslide susceptibility analysis. Geomatics 1(4):399–416
42. Shu H, Guo Z, Qi S, Song D, Pourghasemi H, Ma J (2021) Integrating landslide typology with weighted frequency ratio model for landslide susceptibility mapping: a case study from Lanzhou city of Northwestern China. Remote Sens 13(18):3623. 10.3390/rs13183623
43. Singh AP, Dhadse K, Ahalawat J (2019) Managing water quality of a river using an integrated geographically weighted regression technique with fuzzy decision making model. Environ Monit Assess 191(6):378. 10.1007/s10661-019-7487-z
44. Slingsby JA, Slingsby PW (2019) Monitoring the critically endangered Clanwilliam cedar with freely available Google Earth imagery. PeerJ 7:e7005. 10.7717/peerj.7005
45. Swets JA (1988) Measuring the accuracy of diagnostic systems. Science 240(4857):1285–1293. 10.1126/science.3287615
46. Wang Y, Sun D, Wen H, Zhang H, Zhang F (2020) Comparison of random forest model and frequency ratio model for landslide susceptibility mapping (LSM) in Yunyang County (Chongqing, China). IJERPH 17(12):4206. 10.3390/ijerph17124206
47. Wang X, Nie W, Xie W, Zhang Y (2024) Incremental learning-random forest model-based landslide susceptibility analysis: A case of Ganzhou City, China. Earth Sci Inf 17(2):1645–1661.

https://doi.org/10.1007/s12145-024-01229-2

48. Weigel AP, Liniger MA, Appenzeller C (2008) Can multi-model combination really enhance the prediction skill of probabilistic ensemble forecasts? QJR Meteorol Soc 134(630):241–260. 10.1002/qj.210
49. Williams CJ, Lee SS, Fisher RA, Dickerman LH (1999) A comparison of statistical methods for prenatal screening for Down syndrome. Appl Stoch Models Bus Ind 15(2):89–101. 10.1002/(SICI)1526-4025(199904/06)15:2<89::AID-ASMB366>3.0.CO;2-K
50. Zhao Q, Chen W, Peng C, Wang D, Xue W, Bian H (2022) Modeling landslide susceptibility using an evidential belief function-based multiclass alternating decision tree and logistic model tree. Environ Earth Sci 81(15). 10.1007/s12665-022-10525-3
51. Zimmermann NE, Edwards TC, Graham CH, Pearman PB, Svenning JC (2010) New trends in species distribution modelling. Ecography 33(6):985–989. 10.1111/j.1600-0587.2010.06953.x

Figures

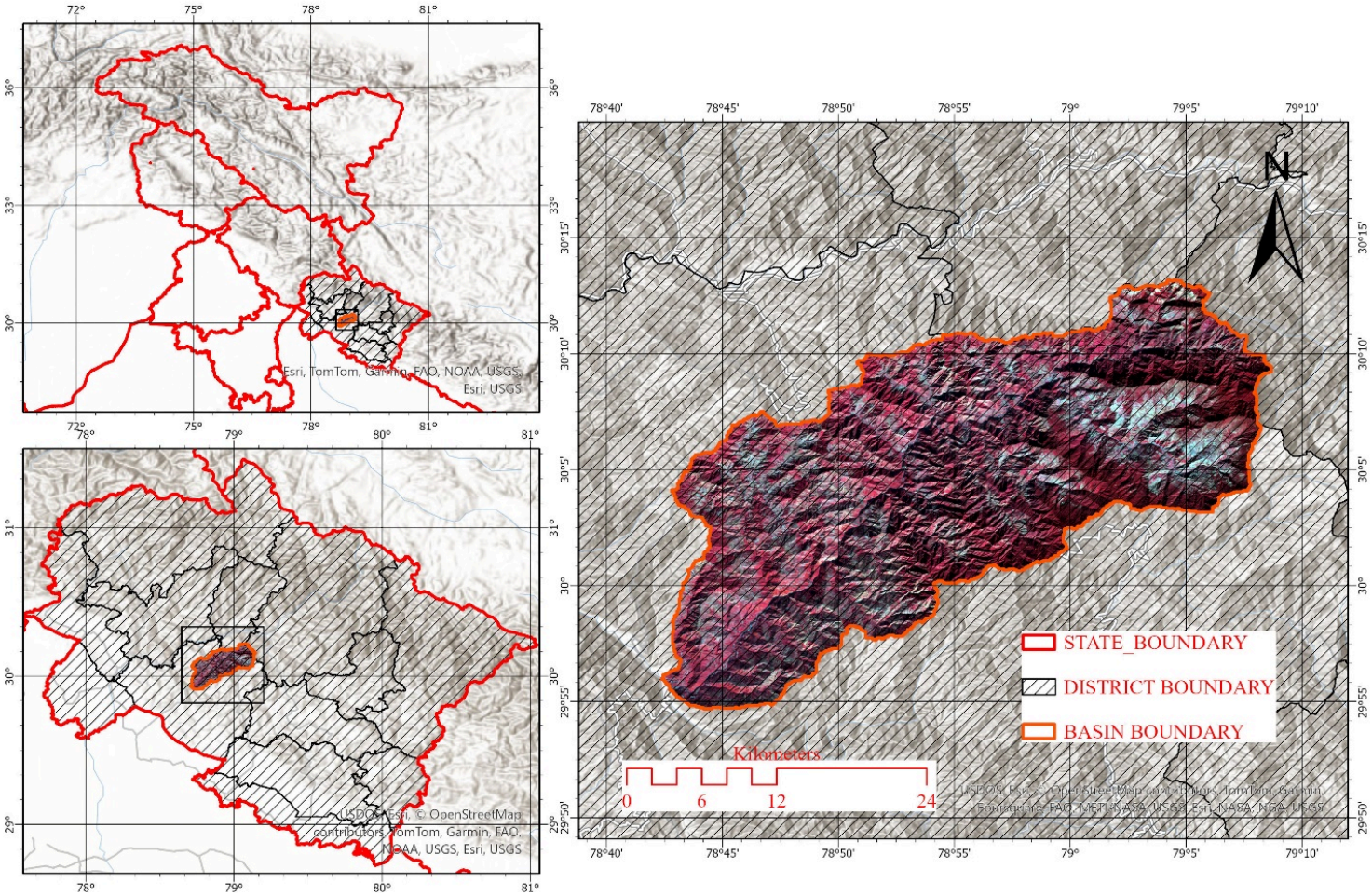

Figure 1

Location Map of the West Nayar Basin, Study area

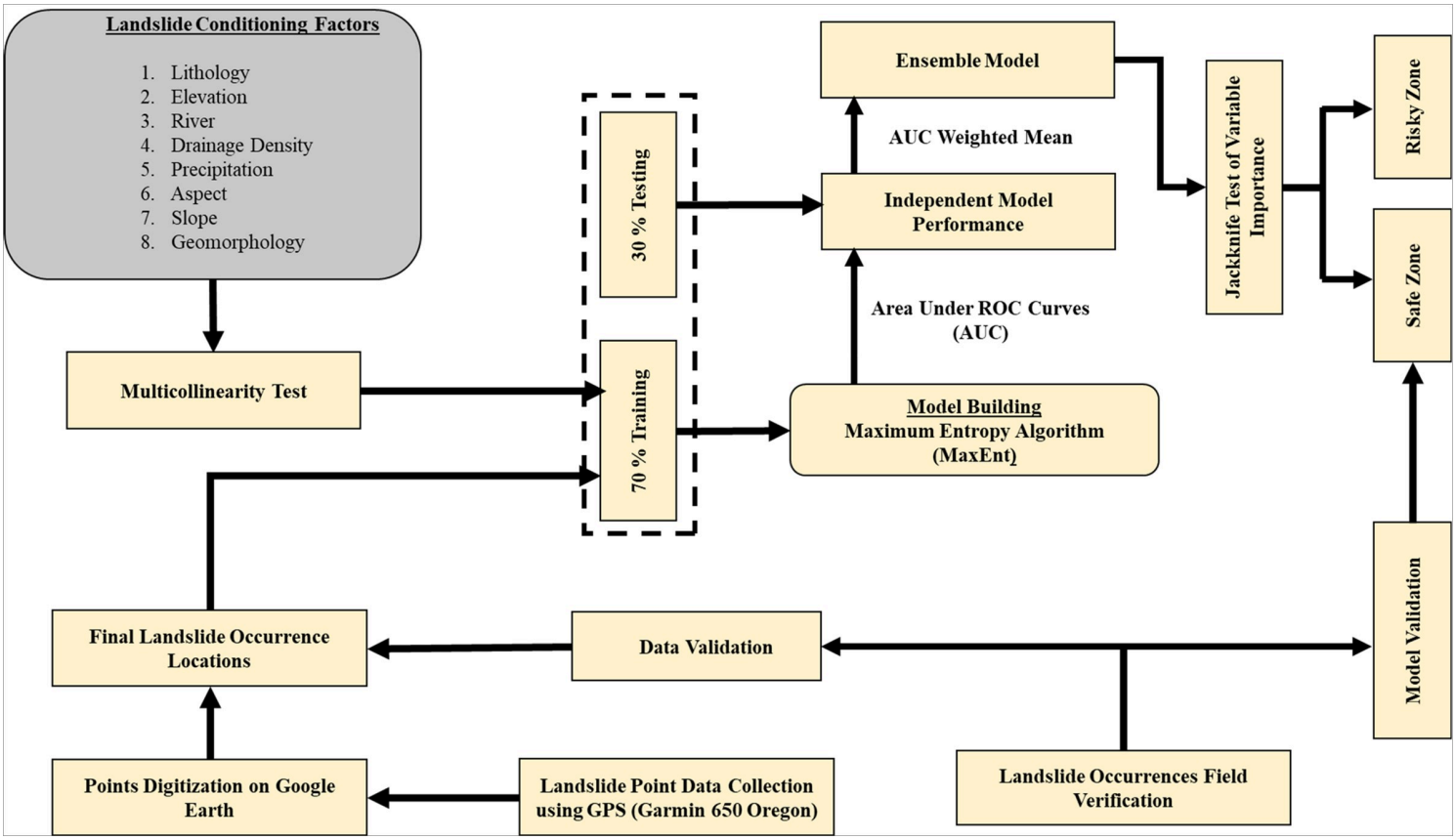

Figure 2

Flow Chart of Research Methodology

Figure 3

Ground Verification and Collecting the Ground Data

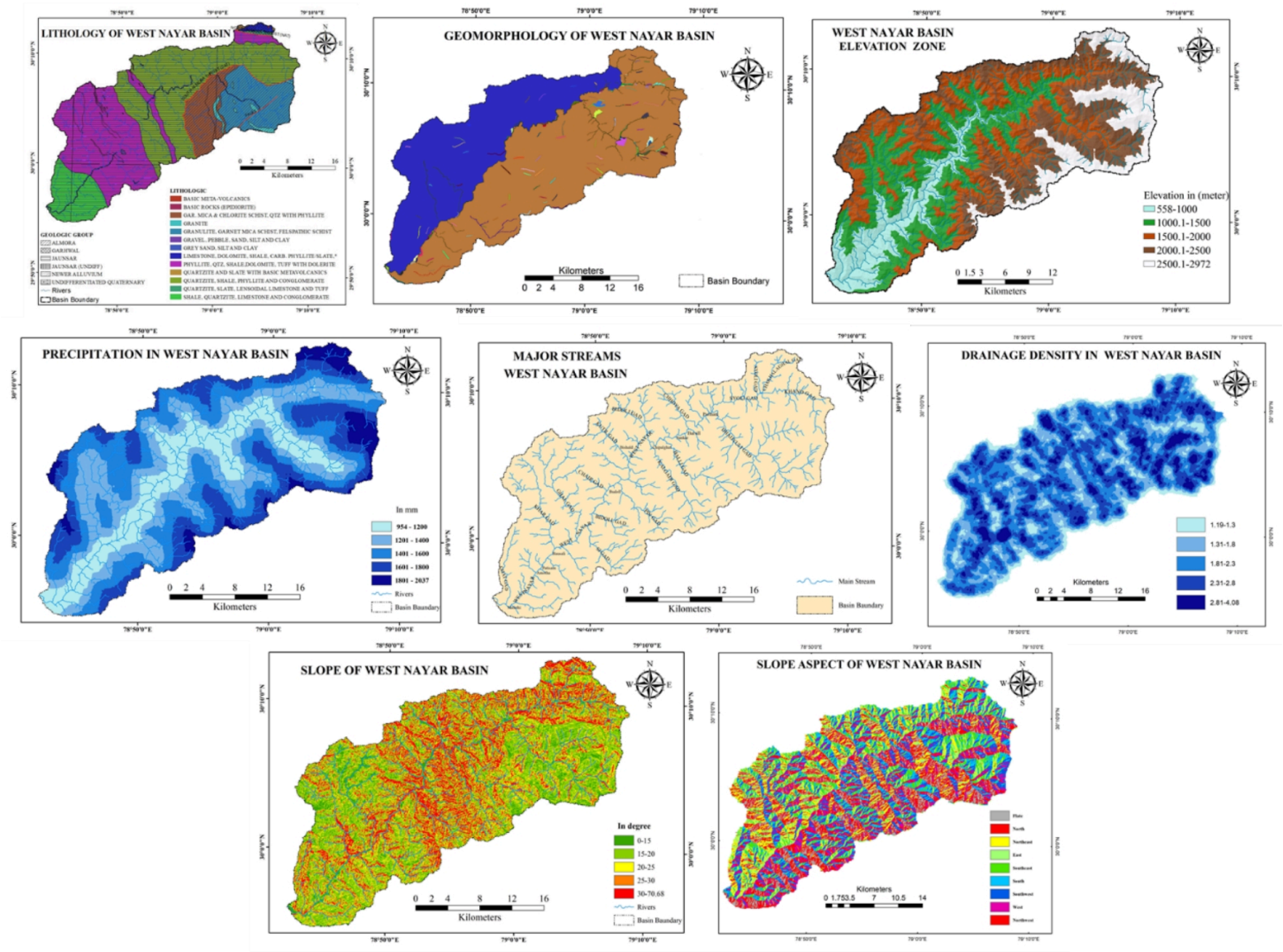

Figure 4 Environmental Variables Lithology, Geomorphology, Elevation, Precipitation, Rivers, Drainage Density, Slope and Aspect

Figure 4

Environmental Variables Lithology, Geomorphology, Elevation, Precipitation, Rivers, Drainage Density, Slope and Aspect

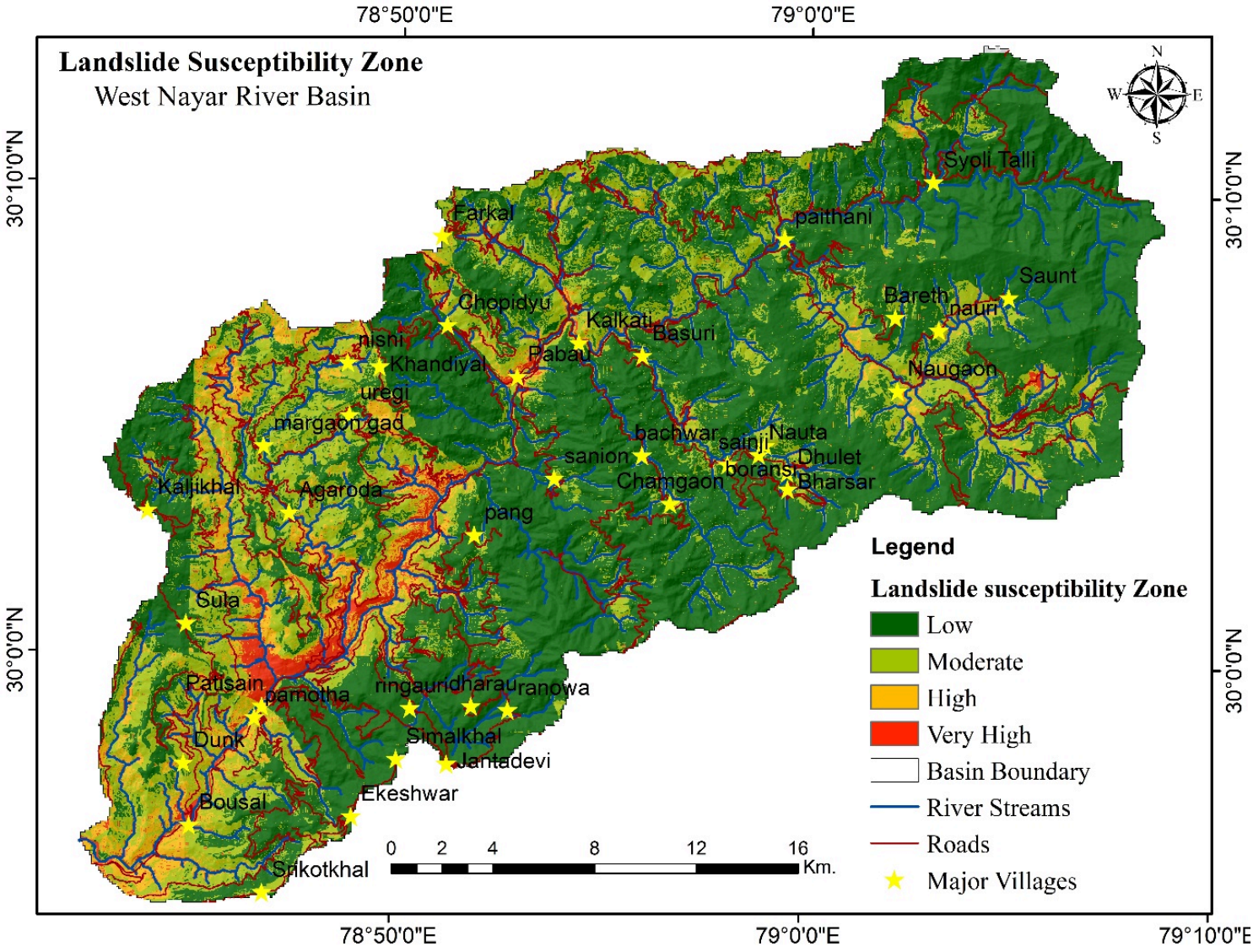

Figure 5

Landslide Susceptibility in West Nayar Basin (WNB)

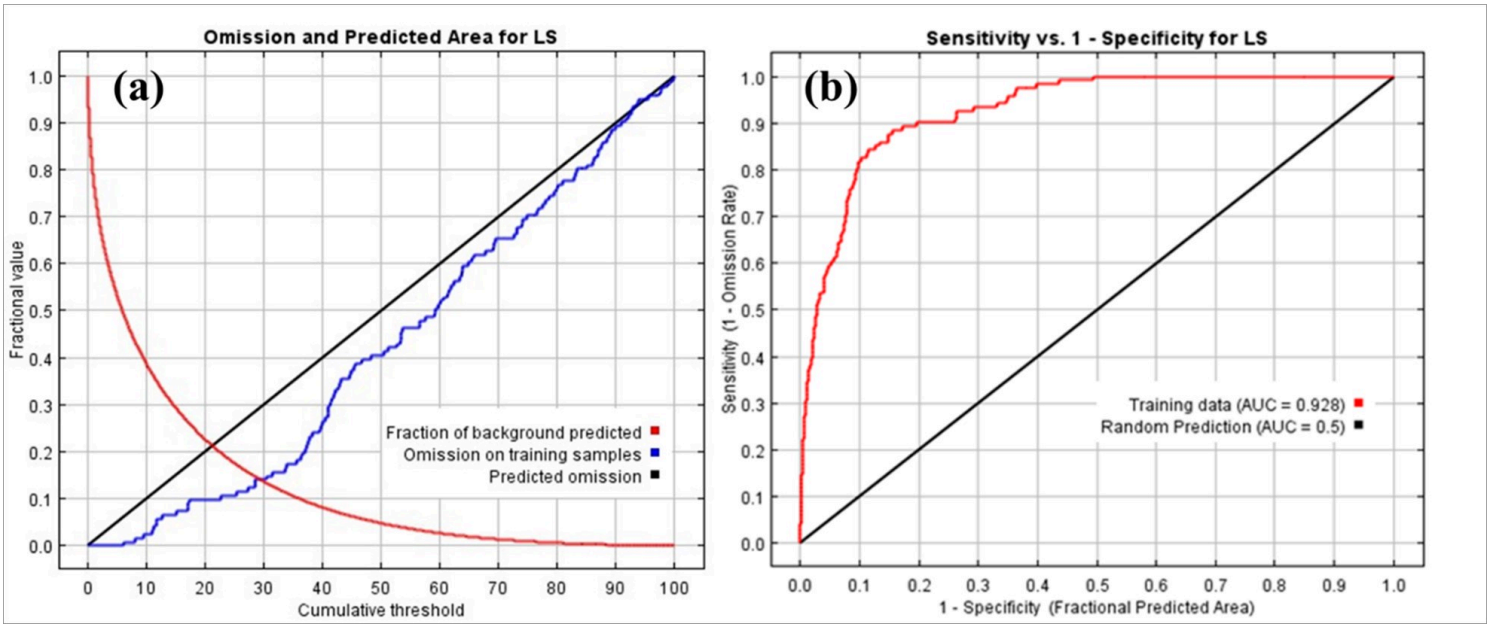

Figure 6

(a) Predictive Performance of MaxEnt Model (b) Receiver Operating Characteristic (ROC) Curve

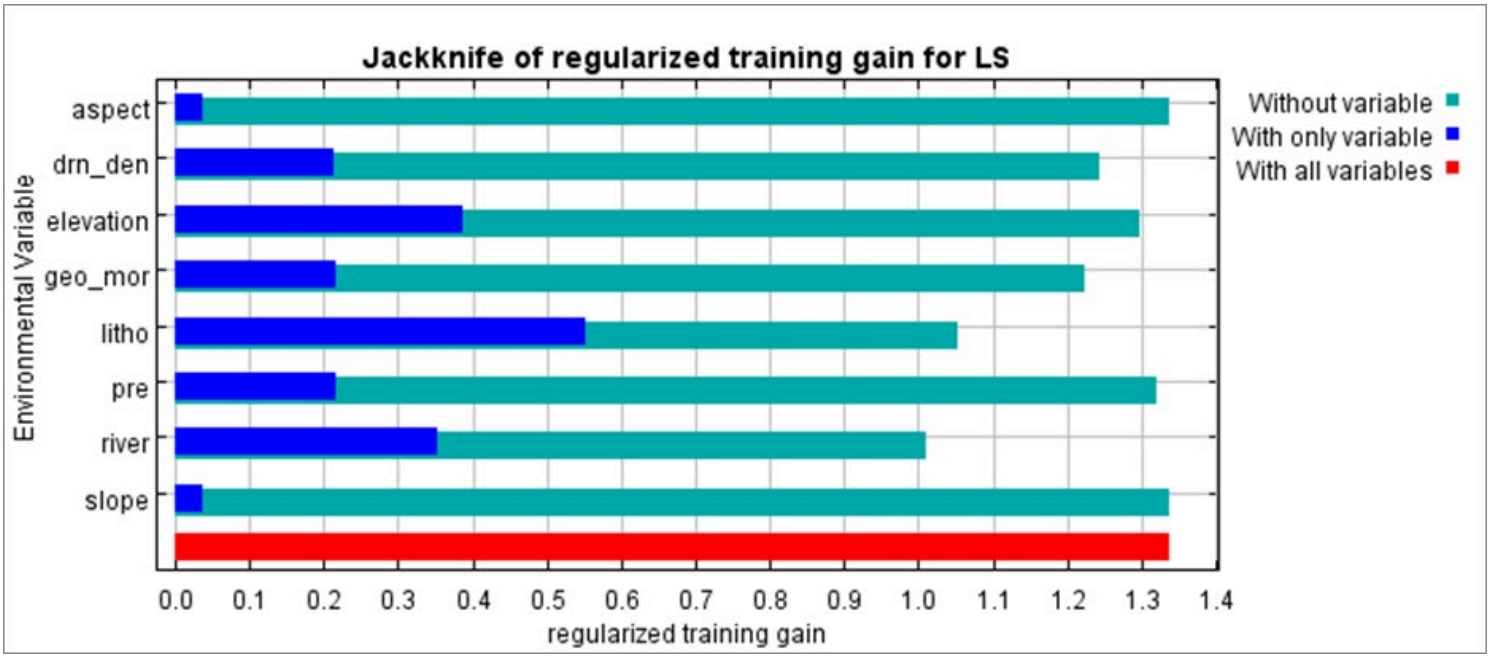

Figure 7

Jackknife Test of Variable Importance

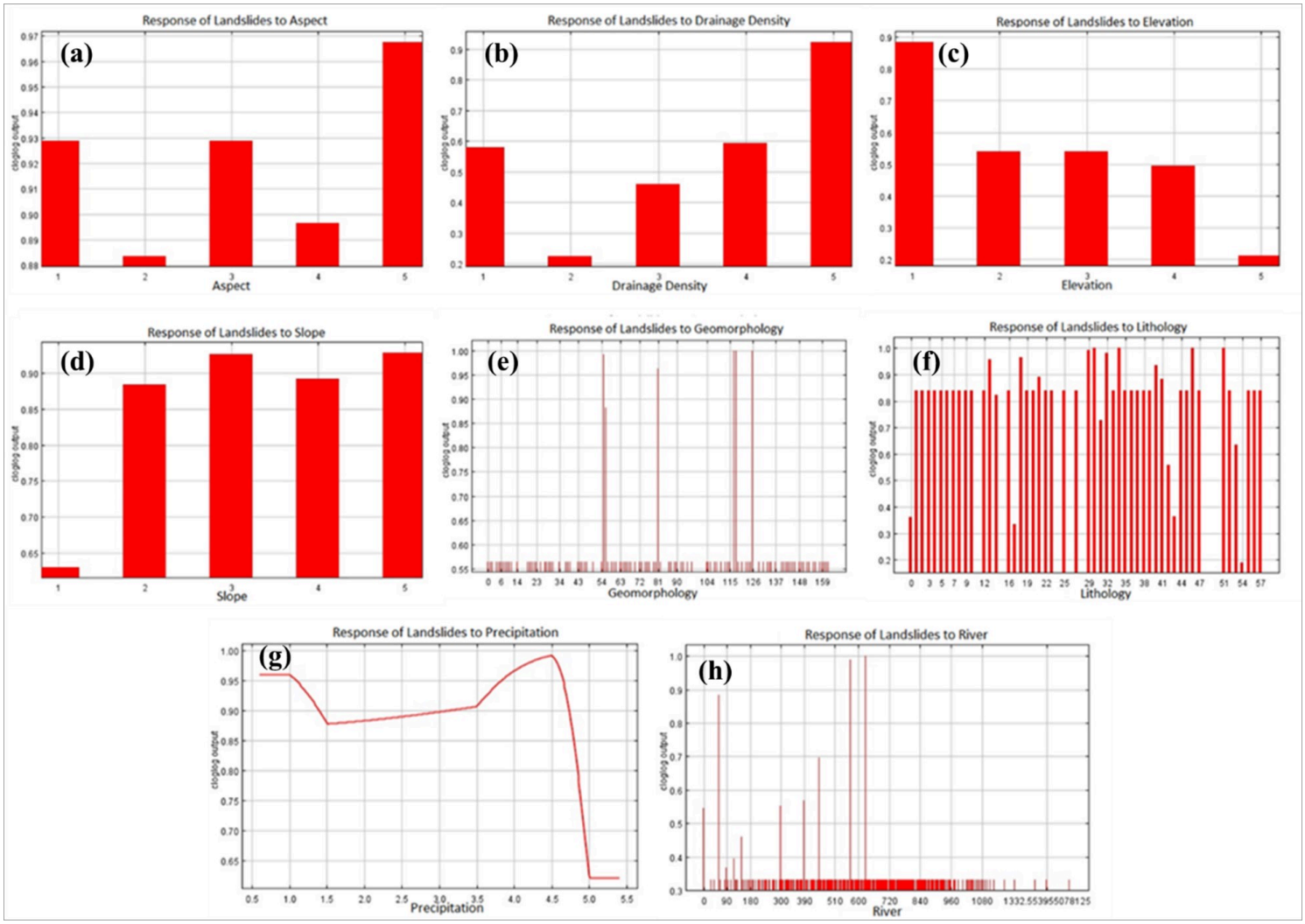

Figure 8

Landslides Response to the (a) Aspect (b) Drainage Density (c) Elevation (d) Slope (e) Geomorphology (f) Lithology (g) Precipitation and (h) River streams